

This is the peer reviewed version of the following article:

Robotic implementation of the slide method for measurement of the thermal emissivity of building elements / Pini, Fabio; Ferrari, Chiara; Libbra, Antonio; Leali, Francesco; Muscio, Alberto. - In: ENERGY AND BUILDINGS. - ISSN 0378-7788. - 114:(2016), pp. 241-246. [10.1016/j.enbuild.2015.07.034]

Terms of use:

The terms and conditions for the reuse of this version of the manuscript are specified in the publishing policy. For all terms of use and more information see the publisher's website.

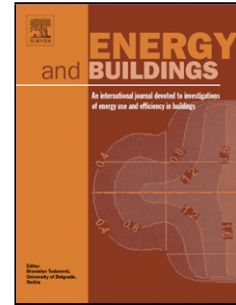
07/10/2024 19:29

(Article begins on next page)

Accepted Manuscript

Title: Robotic implementation of the slide method for measurement of the thermal emissivity of building elements

Author: Fabio Pini Chiara Ferrari Antonio Libbra Francesco Leali Alberto Muscio



PII: S0378-7788(15)30150-X
DOI: <http://dx.doi.org/doi:10.1016/j.enbuild.2015.07.034>
Reference: ENB 6027

To appear in: *ENB*

Received date: 29-4-2015
Revised date: 13-7-2015
Accepted date: 16-7-2015

Please cite this article as: F. Pini, C. Ferrari, A. Libbra, F. Leali, A. Muscio, Robotic implementation of the slide method for measurement of the thermal emissivity of building elements, *Energy and Buildings* (2015), <http://dx.doi.org/10.1016/j.enbuild.2015.07.034>

This is a PDF file of an unedited manuscript that has been accepted for publication. As a service to our customers we are providing this early version of the manuscript. The manuscript will undergo copyediting, typesetting, and review of the resulting proof before it is published in its final form. Please note that during the production process errors may be discovered which could affect the content, and all legal disclaimers that apply to the journal pertain.

1 **Robotic implementation of the slide method**
2 **for measurement of the thermal emissivity of building elements**

3
4

5 Fabio Pini, Chiara Ferrari, Antonio Libbra, Francesco Leali, Alberto Muscio¹
6 Department of Engineering “Enzo Ferrari”, University of Modena and Reggio Emilia, via Vivarelli 10, 41125
7 Modena, Italy

8
9

10 Keywords: emissivity; thermal emittance; infrared emittance; infrared radiation; cool roof;
11 measurement; emissometer; slide method

12
13

14 **ABSTRACT**

15 A significant interest exists in measuring the thermal emissivity of building surfaces since
16 high values combined with high solar reflectance allow rejecting solar energy absorbed by
17 irradiated surfaces, whereas intermediate or low values permit to limit condensation of humidity,
18 heat loss to the sky, or heat transfer through airspaces. The most used measurement method is
19 probably that described by the ASTM C1371 Standard, which correlates the thermal emissivity
20 to the radiative heat flux exchanged in the infrared between the sample surface, kept at ambient
21 temperature, and the bottom surface of a hot emissometer head. With samples showing a low

¹ Corresponding author. Phone: +39 059 2056194; website: www.eelab.unimore.it; email: alberto.muscio@unimore.it (A. Muscio).

22 thermal conductivity, the ‘slide method’ modification is generally used: the hot head is allowed
23 to slide above the sample in order to prevent this from warming up. The slide movement,
24 however, is carried out by hand and time is needed to achieve a stabilized output, therefore the
25 measurement may be time-consuming and also affected by the operator. In order to solve both
26 problems, an automated approach is proposed here, in which the head is moved by the arm of a
27 robot. This manages either the slide movement or the calibration with reference samples,
28 interacting with a computerized data acquisition system that monitors the emissometer output.

29 **Introduction**

30 Thermal emissivity, or thermal emittance, or infrared emittance, is a surface property that
31 represents the ratio of radiant energy emitted in the infrared by a surface and the maximum
32 theoretical emission at the same temperature. It ranges from 0 to 1 or 100%. Measuring the
33 thermal emissivity raises significant interest in the construction sector since a proper choice of its
34 value permits to control the temperature of building surfaces, or heat transfer through such
35 surfaces. It is well known that high values of thermal emissivity allow rejecting solar energy
36 absorbed by irradiated opaque surfaces [1] since in low wind conditions heat transfer to the
37 external environment by infrared radiation is higher than heat transfer with the air by convection.
38 In fact, the performance of opaque building elements in terms of control of solar gains is often
39 expressed through the Solar Reflectance Index (SRI), a parameter defined by the ASTM E1980
40 Standard [2] that combines thermal emissivity with solar reflectance, *i.e.* the surface property
41 representing the fraction of incident solar radiation that is reflected. High values of the SRI,
42 resulting from high values of both solar reflectance and thermal emissivity, are required for solar

43 reflective cool roofing materials, aimed at limiting solar gains through opaque building elements
44 and, consequently, overheating or both single buildings and entire urban areas. In this regard,
45 solar reflectance is the key parameter, but a low thermal emissivity may affect strongly re-
46 emission of the absorbed solar energy and, therefore, the SRI. This is the case of metal surfaces,
47 which can overheat as much as black roofing materials [3-6]. On the other hand, thermal
48 emissivity values lower than those of common non-metallic materials may limit heat loss toward
49 the sky during nighttime or affect the time of humidity condensation [7-8], and they can be
50 desired in case one aims at effects such as limiting excessive cooling and condensation on
51 building surfaces during nighttime. Very low values of thermal emissivity are also exploited to
52 build radiant barriers, including advanced insulation systems such as the so-called multi-
53 reflective radiant barriers [9], aimed at limiting heat transfer by infrared radiation through roofs,
54 air spaces or wall air gaps.

55 In order to assess the energy performance of buildings, thermal emissivity of building
56 surfaces is a parameter that must be known. For an accurate performance assessment, it must be
57 known by measurement. In this regard, several measurement methods are available (see [109] for
58 a review focused on the construction sector, and also [11]), but most methods can be used only in
59 the laboratory, often on small specimens of pure material, therefore they are of low practical
60 usefulness in the construction industry. Only two methods seem available for emissivity
61 measurement on actual building elements, usable either in the laboratory or on field. These are
62 described in the ASTM C1371 Standard Test Method [12] and the EN 15976 Standard [13].
63 ASTM C1371 is probably the most used one, endorsed for performance assessment of solar
64 reflective materials by both the Cool Roof Rating Council of the U.S.A. [14] and the European

65 Cool Roof Council [15] (the latter however allows also EN 15976 after having tested it in an
66 interlaboratory comparison [16]).

67 In the authors' knowledge, only one instrument compliant with ASTM C1371 is
68 commercially available, the Devices & Services AE/RD1 Emissometer. This measures the total
69 hemispherical emissivity of the sample through the following relationship [17]):

$$70 \quad \Delta V = k \cdot \frac{\sigma_0 \cdot (T_d^4 - T^4)}{1/\varepsilon + 1/\varepsilon_d - 1} \equiv f(\varepsilon) \quad (1)$$

71 In the above formula, the voltage signal ΔV [V] returned by a thermopile sensor embedded
72 in the instrument head is proportional by a calibration constant k to the radiative heat flux
73 exchanged between the sample surface and the bottom surface of the head. The first surface has
74 thermal emissivity ε unknown and absolute thermodynamic temperature stabilized at a value T
75 [K] as close as possible to the ambient one, T_a [K]; the second surface has known thermal
76 emissivity ε_d and absolute thermodynamic temperature stabilized at an assigned value T_d [K],
77 significantly higher than that of the analyzed surface or the ambient ($T_d > T \cong T_a$). The calibration
78 constant k multiplies the heat flux exchanged by thermal radiation between the two surfaces,
79 which are assumed to be flat, parallel, virtually infinite and facing each other, as well as gray and
80 diffusive. The emissometer is calibrated before each test by measuring two reference samples
81 with known emissivity, respectively equal to 0.05 and 0.88 in the experiments described here.
82 The samples were provided by the producer of the emissometer, which ensures linearity of the
83 instrument, that is of the correlation between ΔV and ε in the last equality of Eq. (1), and
84 uncertainty ± 0.01 in the range $0.03 \leq \varepsilon \leq 0.93$. The instrument measures something between normal
85 and hemispherical emissivity, nonetheless it was shown to yield the hemispherical emissivity

86 when that of the two reference samples is interpolated [18-19]. While it is a quite simple device,
87 it is largely used in the scientific community and the industry, and studies have been made for its
88 improvement [20-21].

89 If the sample shows a non-negligible resistance to heat transfer, due to a low thermal
90 conductivity of the support material, the heat input applied by the emissometer head to the
91 measured surface causes a thermal gradient across the thickness of the sample itself. As a result,
92 the temperature T of the measured surface rises to a value significantly higher than that of the
93 ambient air, T_a . In this case, the actual value of thermal emissivity can be recovered by using one
94 among the modifications of the standard method suggested by the producer of the emissometer.
95 The most used one is the so-called 'slide method' [22-24], in which the head of the emissometer
96 is allowed to slide above the measured surface in order to prevent the sample from warming up.
97 The sliding operation is carried out by hand and time is needed to achieve a stabilized output of
98 the instrument, therefore the measurement may be time-consuming, and it may also be affected
99 by the operator's expertise. An approach was recently proposed [21] to solve both problems,
100 based on automating the sliding operation by means of a robotized arm. In particular, the
101 emissometer head is moved by the arm of a SCARA robot, which manages either the sliding
102 movement or the calibration with the reference samples. The voltage output returned by the
103 emissometer is acquired by a computerized data acquisition system, which allows visualizing in
104 real time the time-evolution pattern of the measured signal and may also interact with the robot.
105 The approach has eventually provided the encouraging results presented here, with
106 measurements in very good agreement with manual operation and also excellent repeatability.

107 **Experimental Setup and Method**

108 An experimental apparatus has been developed in order to automate the slide method. The
109 apparatus is based on a robotic arm and a PC based Human Machine Interface (PC-HMI). As
110 depicted in Fig. 01, the core of the apparatus is a Mitsubishi RH-5AH55 SCARA robot, #1 in the
111 figure, connected to a MELFA CR2A-572 controller.

112 The arm of the robot has radius of the working volume 0.55 m and maximum payload 5 kg.
113 It handles the measurement head of a Devices & Services AE1 emissometer, #3, through a
114 dedicated holding device, #2. Entering into details, a tailored adapter with vertical compliance
115 has been designed to attach the emissometer head. The top of the adapter is rigidly connected
116 with the cylindrical shaft of the robot arm. Conversely, a spring connects the emissometer head
117 and the compliance adapter to provide continuous contact with the surface of the tested sample.
118 The adapter allows avoiding accurate robot programming and positioning since the spring self-
119 adapts the head to keep it in contact with the sample surface.

120

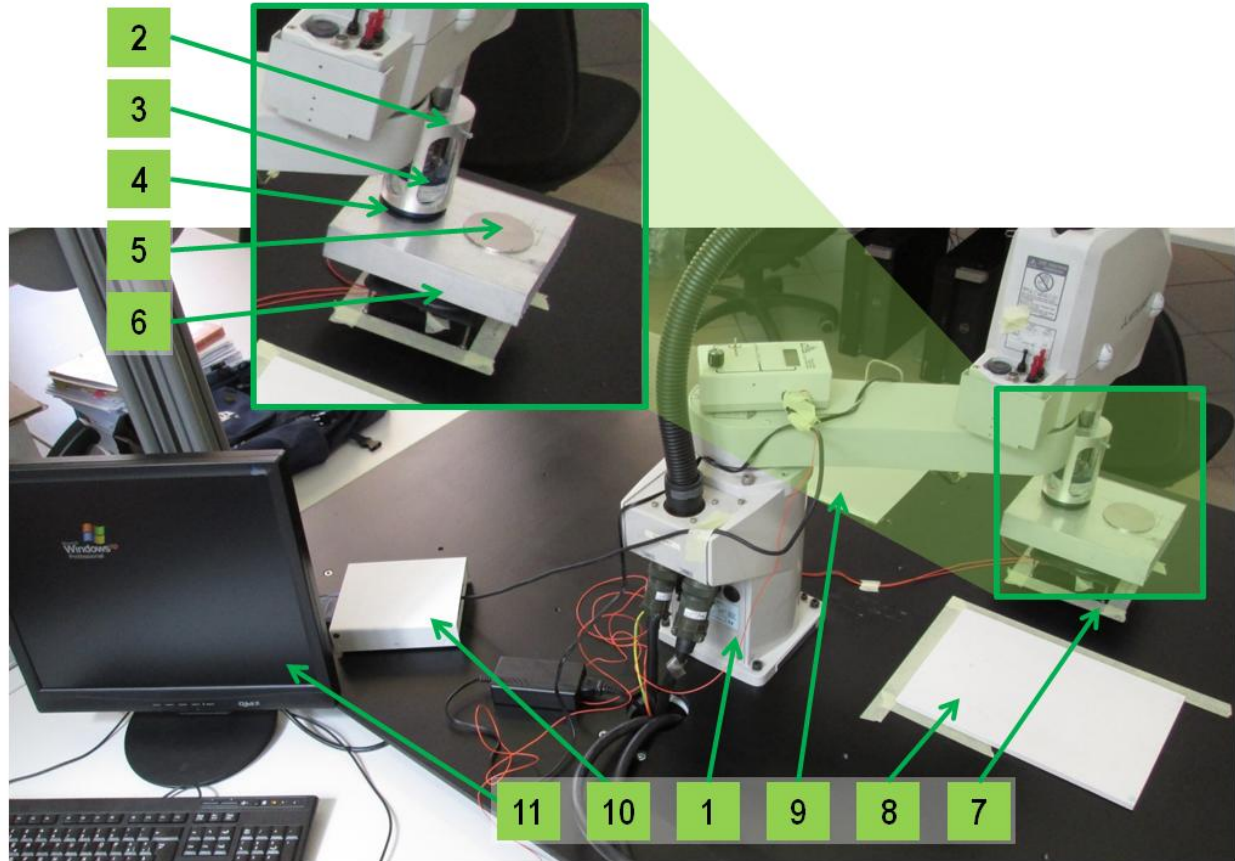


Figure 01. Experimental apparatus.

121
122
123

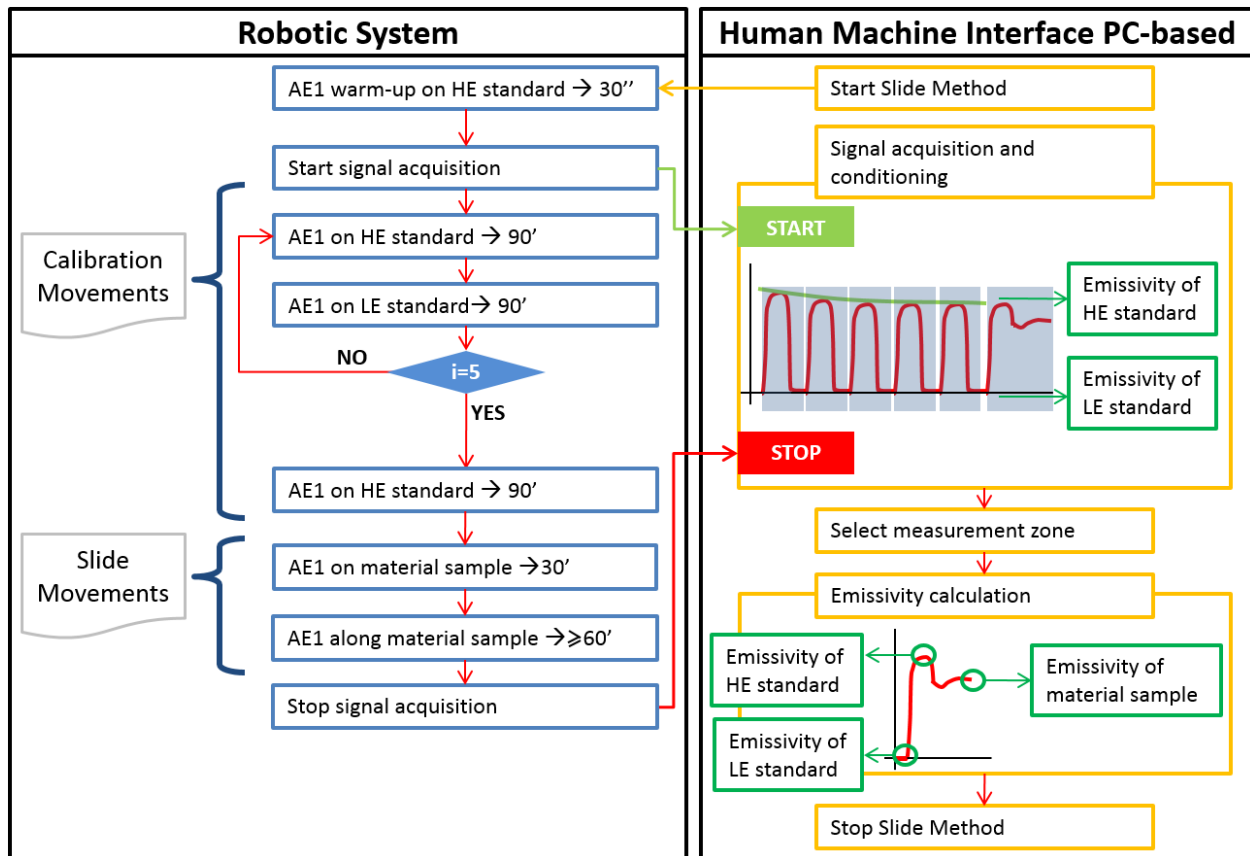
124 The robot workspace is arranged in a calibration area, #7, and two measurement areas, #8
125 and #9. The calibration area locates the High Emissivity standard (HE standard) as #4, and the
126 Low Emissivity standard (LE standard) as #5, on a heat sink provided with the emissometer, #6.
127 A fan placed on the back of the heat sink is employed to improve and keep constant the exchange
128 of heat between heat sink and surrounding air. The measurement areas #8 and #9 are
129 symmetrical with respect to the calibration area #7 and locate the Material Samples (MS) to be
130 tested. The proposed layout reduces the robot movement and allows replacement of a sample
131 during the performance of measurements on the other one.

132 Concerning the PC-HMI, a PC with Windows OS, #11, and a National Instruments Data
133 Acquisition card (DAQ card) PCI-6034E with SCB-68 board, #10, are employed for data
134 acquisition, signal conditioning, and control of the robot.

135 The slide method is implemented by means of a robot control routine and a dedicated
136 software tool. The control routine is run by the robot controller. A first high speed movement is
137 employed to place the emissometer head on the HE and LE standards. In sequence, the robot arm
138 moves the head on the HE standard and keeps it in place for 90 s, thereafter it moves the head on
139 the LE standard and keeps it in place for 90 s. Such sequence is repeated several times until
140 constant voltage values are returned by the head sensor for both standards. In the experimental
141 practice, one warm-up cycle with 5 repetitions was enough. For subsequent measurements only 2
142 repetitions were required.

143 Afterwards, the robot performs the emissometer calibration on the HE standard, and thus
144 starts the movements to execute the slide operation on the tested sample. In particular, the robot
145 moves the emissometer head on a corner of the tested surface and leaves it in contact with the
146 sample for 30 s. Subsequently, the head is moved along the surface following a pattern
147 composed by a sequence of parallel linear movements. Semicircular movements connect the
148 linear trajectories to reduce the acceleration in direction changes. The speed selected for the
149 movements is that minimizing voltage fluctuation of the signal returned by the AE1
150 emissometer, and it is given by an initial stage of sliding on the sample. Figure 02 summarizes
151 the process operation, while Figure 03 shows the sequence of positions of the emissometer head
152 imposed by the robot.

153



154
155

Figure 02. Operations of the robotic slide method.

156

STEP 1 – Calibration on the High Emissivity Standard**STEP 2 – Calibration on the Low Emissivity Standard****STEP 3 – Stop on the sample material****STEP 4 – Slide on the sample material**

157
158

Figure 03. Positions of the emissometer head imposed by the robot.

159

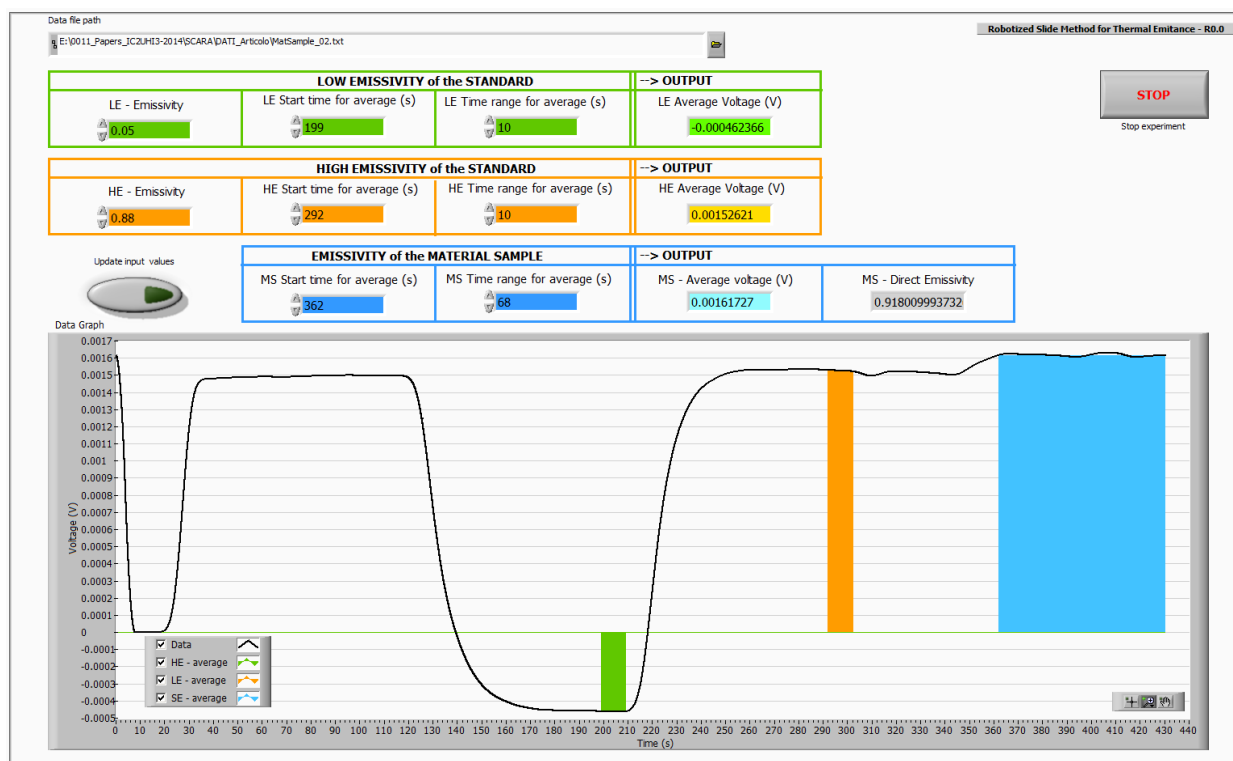


Figure 04. Voltage signal returned by the emissometer and averaging process (sample B).

160
161
162

163 The control PC executes a virtual instrument built in the Labview programming
164 environment, implementing the PC-HMI. The virtual instrument manages the DAQ card and
165 performs data acquisition and signal conditioning. Since synchronization between the control PC
166 and the robot controller is not yet implemented, user interaction is currently required to select the
167 time interval in which the thermal emissivity is calculated from the output voltage signal
168 returned by the thermopile sensor of the emissometer head. Figure 04 shows the PC-HMI while
169 the user manages the time intervals in which the voltage signal is averaged to calculate thermal
170 emissivity. The time intervals are evidenced by different colors (green for the LE standard,
171 orange for the HE standard, pale blue for the measure sample).

172 Comparing the voltage signal returned by the emissometer head while this is positioned on
 173 the measured sample with the signal returned while the head is on the calibration standards
 174 allows determining the sample emissivity.

175 With regard to the direct correlation between the voltage signal returned by the instrument
 176 head and the radiative flux exchanged with the sample surface, and assuming the linear behavior
 177 of the instrument mentioned in the Introduction section, Equation (1) can be simplified as
 178 follows.

$$179 \quad \Delta V = K \cdot \varepsilon + \Delta V_0 \quad (2)$$

180 Equation (2) applies if the emissometer and the analyzed surface have constant
 181 temperatures, condition achieved within a short warm-up phase and thanks to the constant speed
 182 movements of the robot. As a result, Equations (3)-(4)-(5) are valid in the robotic slide method.

$$183 \quad \Delta V_{LE} = K \cdot \varepsilon_{LE} + \Delta V_0 \quad (3)$$

$$184 \quad \Delta V_{HE} = K \cdot \varepsilon_{HE} + \Delta V_0 \quad (4)$$

$$185 \quad \Delta V_{MS} = K \cdot \varepsilon_{MS} + \Delta V_0 \quad (5)$$

186 Equation (3) is related to the LE standard, where ΔV_{LE} [V] is the voltage returned by the
 187 instrument head and ε_{LE} is the emissivity of the standard. Likewise, in Eqs. (4)-(5), ΔV_{HE} [V] and
 188 ΔV_{MS} [V] are the voltages, ε_{HE} and ε_{MS} the thermal emissivities of HE standard and the material
 189 sample (MS) under test, respectively. From the equation set (3)-(5) it is eventually possible to
 190 define the correlation formula between the voltages returned by the emissometer head for the HE
 191 standard, the LE standard and a MS sample, and the corresponding emissivities.

$$192 \quad \varepsilon_{MS} = \varepsilon_{LE} + (\varepsilon_{HE} - \varepsilon_{LE}) \cdot \frac{(\Delta V_{MS} - \Delta V_{LE})}{(\Delta V_{HE} - \Delta V_{LE})} \quad (6)$$

193 **Experimental results**

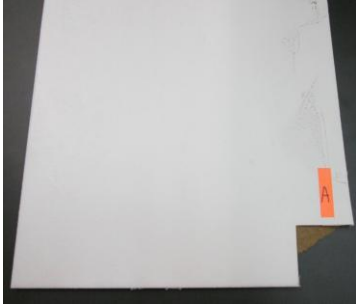
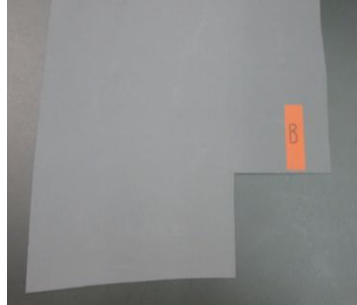




194 In order to evaluate the effectiveness of the robotic implementation of the slide method, the
195 developed apparatus has been employed to measure the thermal emissivity of several samples of
196 commercially available materials. The samples were previously measured through manual
197 execution of the slide method, therefore their emissivity is assumed to be known. Table 1
198 collects pictures of the tested samples and their thermal emissivity as returned by the manual
199 slide measurements performed by experienced operators.

200

201

202

Table 1. Tested material samples.

<p style="text-align: center;">A</p>  <p style="text-align: center;">Coated Masonite board $\epsilon_{manual} = 0.91$</p>	<p style="text-align: center;">B</p>  <p style="text-align: center;">Coated canvas $\epsilon_{manual} = 0.85$</p>	<p style="text-align: center;">C</p>  <p style="text-align: center;">Aluminum plate $\epsilon_{manual} = 0.05$</p>
<p style="text-align: center;">D</p>  <p style="text-align: center;">Veneered chipboard $\epsilon_{manual} = 0.90$</p>	<p style="text-align: center;">E</p>  <p style="text-align: center;">Painted multilayer plate (Al/PE/Al) $\epsilon_{manual} = 0.85$</p>	<p style="text-align: center;">F</p>  <p style="text-align: center;">Painted multilayer plate (Al/PE/Al) $\epsilon_{manual} = 0.87$</p>

203

204 For each sample, six robotic sliding tests have been performed, following an univocal
 205 sequence. The speed adopted for the slide movement was 7 mm/s, with the AE1 emissometer
 206 head slightly pressed on the surface of the sample. For each test, the voltage returned by the AE1
 207 emissometer is collected in a separate file and separately examined by means of the PC-HMI.

208 As an example of the robotic slide measuring process, Table 2 collects data for the material
 209 sample **A**. Data related to the employed time intervals required to calculate the emissivity have
 210 also been collected. The rows of Tab. 2 collects information about start time and time interval

211 settings employed to calculate the average value of the voltage returned by the emissometer. In
 212 sequence, information about measurement on LE standard, HE standard and tested sample are
 213 collected. The last rows of Tab. 2 report the values of average thermal emissivity, standard
 214 deviation and coefficient of variation calculated with the six measurements.

215

216

Table 2. Thermal emissivity evaluation process for material sample A.

MATERIAL SAMPLE A		Measures					
		#1	#2	#3	#4	#5	#6
LE Standard							
Start time for average	[s]	204	201	201	202	199	205
Time range for average	[s]	8	8	8	8	8	8
Average voltage	[V] $\times 10^{-4}$	-2.042	-1.952	-2.123	-2.197	-2.113	-2.077
HE Standard							
Start time for average	[s]	293	292	291	292	291	296
Time range for average	[s]	8	8	8	8	8	8
Average voltage	[V] $\times 10^{-4}$	19.948	19.896	19.781	19.797	20.081	19.812
Material Sample							
Start time for average	[s]	360	360	363	363	359	365
Time range for average	[s]	54	54	54	54	54	54
Average voltage	[V] $\times 10^{-4}$	20.63	20.633	20.508	20.353	20.702	20.423
Emissivity (robotic slide)	[-]	0.905	0.908	0.907	0.901	0.903	0.903
Summary							
Average Emissivity	[-]	0.90					
Standard deviation	[-]	0.003					
Coefficient of variation	%	0.31					

217

218 Following the proposed measuring and calculation method, the comparison between
 219 robotic slide and manual slide along the six material samples treated is presented in Tab. 3. The
 220 three upper rows collect average thermal emissivity, standard deviation and the coefficient of
 221 variation given by the robotic slide. The two bottom rows report the value of thermal emissivity

222 returned by the manual slide and the difference between the thermal emissivity by the robotic
 223 and manual slide. The agreement is indeed very good, mostly within the uncertainty of the
 224 instrument. Repeatability was also excellent.

225

226 Table 3. Thermal emissivity evaluation for material samples **A-F**.

		Material samples					
		A	B	C	D	E	F
Average emissivity (robotic slide)	[-]	0.90	0.84	0.04	0.87	0.85	0.87
Standard deviation	[-]	0.003	0.003	0.004	0.002	0.003	0.003
Coefficient of variation	%	0.31	0.34	9.55	0.19	0.31	0.38
Average emissivity (manual slide)	[-]	0.91	0.85	0.05	0.90	0.85	0.87
Difference (robotic vs manual)	[-]	-0.01	-0.01	-0.01	-0.03	0.00	0.00

227

228 **Conclusive remarks**

229 A robotic implementation has been made of the ‘slide method’ modification of ASTM
 230 C1371 standard test method, aimed at measuring the thermal emissivity at the surface of low-
 231 conductivity materials such as those of typical building elements. The robotic implementation
 232 allows eliminating the man in the loop and improving efficiency and repeatability of
 233 measurements.

234 The robotized slide method returned the same results of the standard, *i.e.* manual, slide
 235 method for several different samples with high and low thermal emissivity. Either accuracy or
 236 repeatability were found to be from very good to excellent, generally returning emissivity
 237 values within the uncertainty declared by the emissometer producer.

238 Future development will implement the full synchronization between the PC running the
239 PC-HMI and the robot controller, in order to manage the robot operation in function of the
240 output signal. Data acquisition with an insulated DAQ card will also be considered to remove
241 some high frequency components of the measured voltage signal due to the robot drives, which
242 are currently filtered. Self-adjustment of the robot speed during execution of the slide movement
243 will also be implemented. Future work will eventually be aimed at simplifying and consolidating
244 the experimental apparatus, in order to obtain a relatively inexpensive and easy to use tool
245 complementing the standard instrument and possibly usable on field.

246

247 **Acknowledgments**

248 The authors wish to acknowledge students Luca Ferrari and Nicola Giannotta for their
249 contribution to development of the experimental setup. This work has been developed with the
250 equipment of laboratories LaPIS (<http://www.robofacturing.unimore.it>) and EELab
251 (<http://www.eelab.unimore.it>) of the University of Modena and Reggio Emilia.

252

253 **References**

- 254 1. R. Levinson, P. Berdahl, H. Akbari, W. Miller, I. Joedicke, J. Reilly, Y. Suzuki, M.
255 Vondran, Methods of creating solar-reflective nonwhite surfaces and their application to
256 residential roofing materials, *Solar Energy Materials & Solar Cells* 91 (2007) 304-314.

- 257 2. ASTM International, E1980-11 – Standard Practice for Calculating Solar Reflectance Index
258 of Horizontal and Low-Sloped Opaque Surfaces, 2011.
- 259 3. A.H. Rosenfeld, H. Akbari, S. Bretz, B.L. Fishman, D.M. Kurn, D. Sailor, H. Taha,
260 Mitigation of urban heat islands: materials, utility programs, updates, *Energy and Buildings*
261 22 (1995) 255-265.
- 262 4. S. Bretz, H. Akbari, A.H. Rosenfeld, Practical issues for using solar-reflective materials to
263 mitigate urban heat islands, *Atmospheric Environment* 32 (1998) 95-101.
- 264 5. A. Libbra, A. Muscio, C. Siligardi, P. Tartarini, Assessment and improvement of the
265 performance of antisolar surfaces and coatings, *Progress in Organic Coatings* 72 (2011) 73-
266 80.
- 267 6. A. Libbra, A. Muscio, C. Siligardi, Energy performance of opaque building elements in
268 summer: Analysis of a simplified calculation method in force in Italy, *Energy and Buildings*
269 64 (2013) 384-394.
- 270 7. A. Synnefa, M. Santamouris, I. Livada, A study of the thermal performance of reflective
271 coatings for the urban environment. *Solar Energy Journal* 80 (2006) 968-981.
- 272 8. M. Santamouris, A. Synnefa, T. Karlessi, Using advanced cool materials in the urban built
273 environment to mitigate heat islands and improve thermal comfort conditions, *Solar Energy*
274 85 (2011) 3085-3102.

- 275 9. F. Miranville, A.H. Fakra, S. Guichard, H. Boyer, J.-P. Praene, D., Bigot, Evaluation of the
276 thermal resistance of a roof-mounted multi-reflective radiant barrier for tropical and humid
277 conditions: Experimental study from field measurements, *Energy and Buildings* 48 (2012)
278 79-90.
- 279 10. R. Albatici, F. Passerini, A.M. Tonelli, S. Gialanella, Assessment of the thermal emissivity
280 value of building materials using an infrared thermovision technique emissometer, *Energy*
281 *and Buildings* 66 (2013) 33-40.
- 282 11. L. Ibos, M. Marchetti, A. Boudenne, S. Dactu, Y. Candau, J. Livet, Infrared emissivity
283 measurement device: principle and applications, *Measurement Science and Technology* 17
284 (2006) 2950-2956.
- 285 12. ASTM International, C1371-04a(2010)e1 – Standard Test Method for Determination of
286 Emittance of Materials Near Room Temperature Using Portable Emissometers, 2010.
- 287 13. EN 15976 – Flexible sheets for waterproofing – Determination of emissivity, 2011.
- 288 14. Cool Roof Rating Council, Product Rating Program – CRRC-1, ver. 2015,
289 <http://www.coolroofs.org> [http://coolroofs.org/documents/CRRC-1_Program_Manual_-](http://coolroofs.org/documents/CRRC-1_Program_Manual_-_2015-04-16.pdf)
290 [_2015-04-16.pdf](http://coolroofs.org/documents/CRRC-1_Program_Manual_-_2015-04-16.pdf)
- 291 15. European Cool Roof Council, Product Rating Manual, ver. November 2014,
292 http://coolroofcouncil.eu/files/PRP/ECRC_Product_rating_manual.pdf

- 293 16. A. Synnefa, A. Pantazaras, M. Santamouris, E. Bozonnet, M. Doya, M. Zinzi, A. Muscio, A.
294 Libbra, C. Ferrari, V. Coccia, F. Rossi, D. Kolokotsa, Interlaboratory comparison of cool
295 roofing material measurement methods, Proc. 34th AIVC – 3rd TightVent – 2nd Cool Roofs' –
296 1st venticool Conferences, Athens (2013) 52-54.
- 297 17. Devices & Services Co., D&S Technical Note 79-17 – Emissivity measurements for in place
298 surfaces and for materials with low thermal conductivity, 1979,
299 http://www.devicesandservices.com/technical_notes.htm
- 300 18. T.G. Kollie, F.J. Weaver, D.L. McElroy, Evaluation of a commercial, portable, ambient
301 temperature emissometer, Review of Scientific Instruments 61 (1990) 1509-1517.
- 302 19. Devices & Services Co., D&S Technical Note 92-11 – Emissometer Model AE –
303 Hemispherical vs Normal Emittance, 1992,
304 http://www.devicesandservices.com/technical_notes.htm
- 305 20. Y.-C.M. Li, Improved uncertainty for a modified commercial emissometer, Solar Energy
306 Materials & Solar Cells 91 (2007) 735-739.
- 307 21. F. Pini, C. Ferrari, A. Libbra, F. Leali, A. Muscio, Robotic implementation of the slide
308 method for measurement of thermal emittance, Proc. 3rd Int. Conf. on Countermeasures to
309 Urban Heat Island (2014) 457-464.
- 310 22. Devices & Services Co., D&S Technical Note 04-1 – Emissometer model AE – Slide
311 Method for AE Measurements, 2004,
312 http://www.devicesandservices.com/technical_notes.htm

- 313 23. Devices & Services Co., D&S Technical Note 10-2 – Emissometer model AE1 – Slide
314 Method for High Emittance Materials with Low Thermal Conductivity, 2010,
315 http://www.devicesandservices.com/technical_notes.htm
- 316 24. Devices & Services Co., D&S Technical Note 11-2 – Model AE1 Emittance Measurements
317 using a Port Adapter, Model AE-ADP, 2011,
318 http://www.devicesandservices.com/technical_notes.htm

Robotic implementation of the slide method for measurement of the thermal emissivity of building elements

Fabio Pini, Chiara Ferrari, Antonio Libbra, Francesco Leali, Alberto Muscio*

Department of Engineering “Enzo Ferrari”, University of Modena and Reggio Emilia, via Vivarelli 10, 41125 Modena,
Italy

*Corresponding author: ¹ Phone: +39 059 2056194; website: www.eelab.unimore.it; email:
alberto.muscio@unimore.it (A. Muscio).

HIGHLIGHTS

- Thermal emissivity, or emittance, is a key property for heat transfer of building surfaces
- For accurate assessment of building performance, it must be known by measurement.
- The most used measurement method with low thermal conductivity materials is the ‘slide method’ modification of ASTM C1371.
- The slide operation, performed by hand, may be time-consuming and affected by the operator.
- A robotized version of the slide method has been developed to eliminate the man in the loop.